

UV curing and sol-gel based chemistry: towards nanocomposite coatings in a one step process

Céline Croutxé-Barghorn¹, Cindy Belon, Abraham Chemtob
Department of Photochemistry,
University of Haute-Alsace, ENSCMu,
3, rue Alfred Werner 68093 Mulhouse Cedex, France*

Abstract

The synthesis of organic-inorganic sol-gel coatings was performed using alkoxy silanes bearing either an epoxy or a methacrylate reactive function. These hybrid materials combine numerous advantages such as good adhesion to substrates, abrasion and chemical resistance. Usually, they are synthesized through the successive conventional sol-gel process and organic polymerization. This paper first presents an original organic-inorganic one-step synthesis of ambifunctional alkoxy silane precursors bearing an epoxy or methacrylate function. The UV-generated Brønsted acids from a cationic photoinitiator (PI) were found to be effective in catalyzing alkoxy silane sol-gel polycondensation reactions and initiating the ring-opening reaction of the epoxy functions of TRIMO. Combination of both a radical and a cationic photoinitiator enabled the dual cure of a methacrylate organoalkoxy silane precursor (MAPTMS). These bifunctional hybrid precursors were then mixed with organic resins and the corresponding coatings were characterized. Competition between the formation of inorganic and organic networks was studied using Fourier transform infrared spectroscopy (FTIR). ²⁹Si solid state NMR measurements and thermo-mechanical analyses were also performed with a view to correlate structure and properties of the UV-cured hybrid coatings.

I. Introduction

UV-curing technology and hybrid materials chemistry have recently been combined, opening up new opportunities in the field of UV-cured coatings. The applications targeted include fabrication of waveguide devices ¹⁻³, diffraction gratings ⁴, abrasion resistant coatings ^{5,6} and protective films ⁷⁻⁹. Until now, hybrid sol-gel photomaterials based on epoxy or methacrylate trialkoxy silanes have mostly been synthesized through a two-step process: a

* Celine.Croutxe-Barghorn@uha.fr; tel: + 33 389 335 017; fax: + 33 389 335 014

preliminary sol-gel step led to a liquid organic-based polysiloxane network that was photopolymerized subsequently in presence of a photoinitiator (PI), affording a solid crosslinked organic-inorganic system¹⁰⁻¹³. Nevertheless, few papers have mentioned the synthesis of inorganic oxo-silica networks through a photoacid-catalysed sol-gel process¹⁴⁻¹⁶: hydrolysis and condensation of the reactive silanes took place through the *in situ* liberation of protic acids via the cationic PI photolysis. The only essential feature that distinguishes the photoinduced process from the classical sol-gel route is that no addition of water is required since the simple diffusion of air moisture is enough for the hydrolysis of trialkoxysilyl functions. Compared to a conventional sol-gel process, the UV-induced reaction enables the rapid formation of an oxo-silica film at room temperature in absence of solvent.

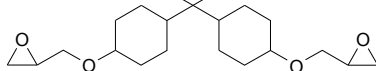
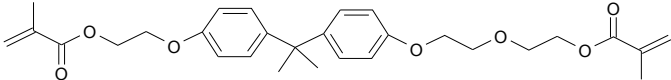
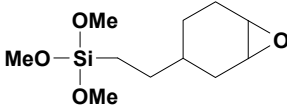
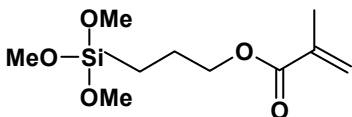
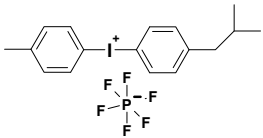
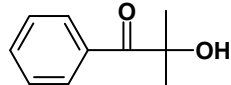
In this paper, we present the one-step UV-curing of cationic or radical bifunctional hybrid precursors bearing both an organic function and alkoxy silane moieties. In a second part, variable amount of these hybrid sol-gel precursors were mixed with an organic reactive resin (EPALLOY 5000 or Sr348c). Sol-gel reactions were catalyzed by the cationic PI and epoxy or methacrylate organic polymerizations initiated concomitantly by the cationic or radical PI respectively. Fourier Transform Infrared spectroscopy (FTIR) was implemented to monitor the dual organic and inorganic reactions. The resulting nanostructured silica-based hybrid films were characterized using ²⁹Si solid state NMR spectroscopy and thermo-mechanical analyses (DMA, scratch test, nanoindentation).

II. Experimental part

II.1 Materials and preparation of hybrid sol-gel films

The cationic and radical hybrid precursors were [2-(3,4-epoxycyclohexyl)ethyl] trimethoxysilane (TRIMO, ABCR) and 3-(methacryloyloxy)propyl trimethoxysilane (MAPTMS, Aldrich) respectively. The cationic resin: hydrogenated diglycidyl ether of Bisphenol A (EPALLOY 5000, CVC Chemicals) and the radical resin: ethoxylated₃ bisphenol A dimethacrylate (Sr348c, Sartomer) were used without further purification. The photoinitiators used in this study were the (4-methylphenyl)[4-(2-methylpropyl) phenyl] iodonium hexafluorophosphate (cationic PI, I 250, Ciba Specialty Chemicals) and the 2-Hydroxy-2-methyl-1-phenyl-propan-1-one (radical PI, D 1173, Ciba Specialty Chemicals). A surface wetting agent (Byk 333, BYK Chemie) was also introduced in the formulations. The structure of the respective monomers and photoinitiators are shown in Table 1.

Table 1: Structure of the monomers and photoinitiators

FUNCTION	COMPOUND	STRUCTURE
Organic monomers	Hydrogenated diglycidyl ether of Bisphenol A EPALLOY 5000	
	Ethoxylated ₃ bisphenol A dimethacrylate Sr348c	
Hybrid monomers	[2-(3,4-epoxycyclohexyl)ethyl] trimethoxysilane TRIMO	
	3-(methacryloyloxy)propyl trimethoxysilane MAPTMS	
Photoinitiators	(4-methylphenyl)[4-(2-methylpropyl) phenyl] iodonium hexafluorophosphate I 250	
	2-Hydroxy-2-methyl-1-phenylpropan-1-one D 1173	

Two kinds of formulation were prepared for this study: the first one consists of hybrid precursor alone and the second one includes a blend of hybrid precursor and organic monomer. In the paper, E_xT_y (S_xM_y) corresponds to a sample including x wt % of EPALLOY 5000 and y wt % of TRIMO (x wt % of Sr348c and y wt % of MAPTMS). The relative weight compositions of the formulations are reported in the Table below. For both systems, an effective coating thickness of 15 μm was taken.

Table 2 : Composition (wt %) of the UV-curable formulations.

		I 250	D 1173	BYK 333
Hybrid precursor alone	T_{100}	2	-	0.3
	M_{100}	2	2	0.5
Blend of hybrid precursor and monomer	E_xT_y ($x \neq 0$)	2	-	0.3
	S_xM_y ($x \neq 0$)	2 (0 if $x=100$)	2	0.5

II.2 Photopolymerization procedure

The photosensitive materials were spread onto glass plates or BaF₂ chips and the curing was then performed using an UV conveyor system from Qurtech equipped with a H-bulb lamp (Fusion UV systems). The samples were passed successively 5 times under the lamp. In these conditions, the light dose received by the samples is 7.3 J/cm² (UVA: 2.25 J/cm², UVB: 2.1 J/cm², UVC: 0.45 J/cm² and UVV: 2.5 J/cm²). All polymerization experiments were performed under a relative humidity comprised between 30 and 40 %.

II.3 FTIR spectroscopy

The epoxy, methacrylate and methoxysilane conversions after UV-curing were determined by FTIR spectroscopy. For these measurements, the formulations were applied onto a BaF₂ chip which is transparent to IR radiations. A spectrophotometer Bruker Vertex 70 equipped with a DTGS detector with a spectral resolution of 4 cm⁻¹ was used to monitor FTIR spectrum before and after irradiation. The decay of the IR bands at 2840 cm⁻¹ (corresponding to CH₃ symmetric stretch in Si-O-CH₃) was monitored to determine the Si-O-Me hydrolysis conversion. The band at 1310 cm⁻¹ (corresponding to the =CH₂ deformation vibration) was used to evaluate the methacrylate conversion, the one at 885 cm⁻¹ (corresponding to asymmetrical ring stretch vibration) for the epoxy cyclohexyl conversion and the one at 3050 cm⁻¹ (C-H epoxy stretch) for the glycidylether conversion.

II.4 NMR spectroscopy

²⁹Si Solid state NMR measurements were performed on a Bruker MSL 400-spectrometer. Either Single Pulse Magic Angle Spinning (SPE-MAS) or Cross Polarization Magic Angle Spinning (CP-MAS) experiments were performed ensuring the respective quantitative or semi-quantitative determination of the proportions of the Tⁿ Si substructures.

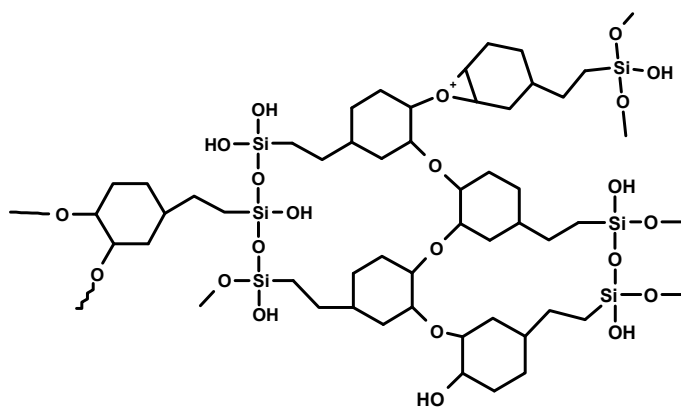
II.5 Thermo-mechanical analysis

The dynamic thermo-mechanical properties of the UV-cured hybrid materials were investigated with a Q800 DMA (TA Instruments) in the tensile configuration. Temperatures ranged from 0 to 260 °C and the heating rate was set at 3 °C/min. The amplitude and frequency of the oscillatory deformations were adjusted to 5 μm and 1 Hz respectively. The scratch resistance of the UV-cured coatings deposited onto glass plate was characterized at room temperature using the apparatus described in previous papers¹⁷. The tip was a 116 μm diameter diamond sphere, the sliding speed was maintained constant (0.03 mm/s) while the normal load was ramped up in steps. The normal loads necessary to delaminate or crack the coatings were reported and the geometry of the grooves created were analysed by an in-situ microscope equipped with a CCD camera. Finally, Hardness (*H*) of the UV-cured coatings were measured with a nanoindenter (CSM Instrument) equipped with a diamond Berkovich indenter (Oliver and Pharr method). Dynamical indentations were performed at a frequency of 1 Hz. A maximal depth of 1 μm was reached and the load was kept for 10 sec before unloading. The residual depth after complete unload was also reported, it gave an insight into the viscoelastic property of the materials.

III. Results and discussion

III.1 Hybrid precursors

The TRIMO precursor was irradiated in presence of a cationic PI (I 250) only. Indeed, the photolysis of the cationic PI generated the powerful superacid HPF_6 , enabling both the epoxy ring-opening and the photoacid-catalyzed sol-gel process. In the MAPTMS case, the cationic PI was combined with a radical PI (D 1173). While I 250 catalyzed the sol-gel process, the D 1173 was necessary to initiate the organic crosslinking. Scheme 1 presents an idealized structure of the TRIMO organic-inorganic network; a similar scheme can be drawn for MAPTMS. In both cases, transparent and homogeneous films were obtained.



Scheme 1: Organic-inorganic hybrid network formed by the dual photocrosslinking of TRIMO alone.

The following table gathers the FTIR and NMR results obtained for the UV-cured hybrid coatings.

Table 3: Organic and inorganic conversions and T^n Si substructures of the 15 μm -thick cured films (after 5 passes under the belt conveyor).

	Epoxy or <u>Methacrylate</u> Conversion (%)	Methoxysilane Hydrolysis Conversion (%)	T^n species * (%)
T_{100}	100	68	T^1 : 24 T^2 : 69 T^3 : 7
M_{100}	58	98	T^1 : 2 T^2 : 55 T^3 : 43

* T^i indicates the fraction of the units with (i) siloxane bonds $-\text{O}-\text{Si}-$ attached to the central silicon.

FTIR results depicted in Table 3 clearly show that both parts of the precursor reacted upon UV exposure. In the TRIMO case, methoxysilane conversion rate reached 68 % and epoxy conversion 100% whereas in the MAPTMS case, methoxysilane conversion was almost complete and methacrylate conversion levelled at 58 %. In addition, the MAPTMS inorganic network was made up mainly of T² and T³ siloxanes sub-structures. This result clearly proves that UV-generated Brönsted acids were efficient in promoting sol-gel condensation reactions. In comparison, TRIMO exhibited a lower degree of condensation (T¹ = 24 %, T² = 69 % and T³ = 7 %): its higher organic reactivity seems to cause an early vitrification of the system that hinders the progress of the sol-gel reactions. Moreover, gel formation is likely to be hindered by the bulky cyclohexyl substituent of this trialkoxysilane.

III.2 Blends of hybrid precursor and monomer

The single-step UV-curing procedure was extended to hybrid organic/inorganic mixture obtained by adding a variable amount of the hybrid precursor (TRIMO or MAPTMS) to a commercial organic resin (EPALLOY 5000 or Sr348c respectively). Owing to the reactive silane's high solubility with the organic resin, high inorganic contents can be achieved in the nanocomposite films. Again, both the organic polymerization and the photoacid-catalyzed sol-gel process took place concomitantly allowing the synthesis of a cross-linked organic photopolymer covalently bound to a siloxane oxo-polymer network. In addition, organic functions from the hybrid precursor can copolymerize with those of the organic resin, thereby providing bonding between the organic and the inorganic phases. A representation of the resultant UV-cured hybrid network is sketched in Scheme 2.



Scheme 2: Organic-inorganic hybrid network formed by the dual UV-curing of an hybrid monomer and organic monomer mixture.

Structural and mechanical investigations were performed on these UV-cured films and the resulting data reported in the following Table:

Table 4: Organic conversions (TRIMO epoxy cyclohexyl function conversions are reported in brackets), Tⁿ Si substructures, glass transition temperatures (T_g) and scratch tests results for the 15 μm-thick cured films (after 5 passes under the belt conveyor).

		Epoxy or methacrylate conversion (%)	T ⁿ species (%)	T _g DMA (°C)	Fn (N) necessary to delaminate	Fn (N) necessary to crack
cationic	E ₁₀₀	79	-	97	0.85	1.19
	E ₈₀ T ₂₀	79 (100)	T ¹ : 47 T ² : 49 T ³ : 4	95	1.09	1.43
	E ₅₀ T ₅₀	78 (100)	T ¹ : 47 T ² : 50 T ³ : 3	120	1.31	1.53
radical	S ₁₀₀	77	-	133	0.73	2.06
	S ₈₀ M ₂₀	90	T ⁰ : 4 T ¹ : 38 T ² : 52 T ³ : 6	183	1.59	1.80
	S ₅₀ M ₅₀	79	T ¹ : 20 T ² : 68 T ³ : 12	-	2.36	2.66

In the present case, the Si-O-Me characteristic band is not usable any more; nevertheless it is still possible to follow the organic conversion of epoxy and methacrylate functions which are expected to be modified by the simultaneous formation of the inorganic network. Indeed, hydroxyl-containing byproducts of the sol-gel reaction (methanol and water) could have an impact the polymerization mechanism thereby affecting the structure of the polymer backbone. Moreover, inorganic network crosslinking might result in an early vitrification and a reduction of the active chains mobility. Lastly, methacrylate photopolymerization being sensitive to atmospheric oxygen, any change in sample viscosity could also affect the polymerization mechanism. In spite of all these parameters, organic conversion rates were not significantly modified by the addition hybrid precursor. The relatively high reactivity of the organic moiety compared to the inorganic hydrolysis and condensation reactions may account for this result. Interestingly, the degree of condensation of the MAPTMS inorganic network was clearly modified by the amount of MAPTMS introduced in the formulation. Indeed, a higher concentration in MAPTMS induces a lower viscosity of the coating that may facilitate the environmental moisture diffusion throughout the film thus improving the efficiency of photoacid catalyzed crosslinking of alkoxy silane. Surprisingly, in the cationic case, the inorganic crosslinking was independent of the TRIMO concentration. The rapid polymerization of the rigid cyclohexyl epoxy functions might result in a decrease in the chains mobility that could hinder the inorganic

condensation to progress. In both radical and cationic cases, the glass transition temperature (T_g) increased with the addition of hybrid precursor. Indeed, the simultaneous formation of the inorganic network probably resulted in an increase in crosslinking density and thus in T_g . The $M_{50}S_{50}$ film was even too rigid to be analyzed by DMA. Scratch tests disclosed that the addition of organo alkoxysilane precursors resulted in the improvement of the adhesion to the glass substrate since the normal load necessary to delaminate the coating increased. This result was expected as alkoxysilanes are coupling agents that provide stable Si-O-Si bonds at the interface between the glass substrate and the organic film. In addition, hybrid films exhibited a higher scratch resistance. Their high stiffness preventing the tip penetration may account for this result.

Figure 1 which displays in-situ pictures of the moving tip taken during the scratch tests performed onto S_{100} and $S_{50}M_{50}$ clearly highlights the better scratch resistance of the hybrid coating compared to the organic one. Under low load ($F_N = 0.2$ N), the deformation generated by the tip left a slight residual plastic groove in the S_{100} case whereas it was still elastic for the hybrid film (the scratch recovered immediately). Finally, at 2.1 N, cracks appeared within the organic film while the hybrid film was still not damaged.

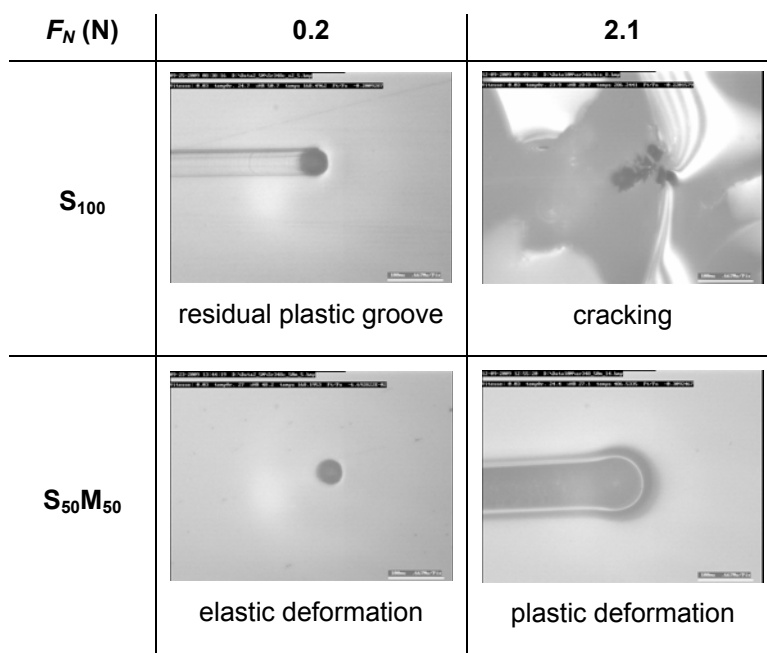


Figure 1: Selected in situ photographs of the moving tip during the increasing normal load scratch performed onto S_{100} and $S_{50}M_{50}$ UV-cured coatings.

In addition to scratch tests, nanoindentation experiments were performed on the S_{100} , $S_{80}M_{20}$ and $S_{50}M_{50}$ cured coatings (Figure 2). The hardness of the films appeared to increase with the content in hybrid precursor. This result corroborates the other thermo-mechanical tests: the higher crosslinking density obtained through the addition of hybrid precursor to organic resin resulted in an increase in the film hardness. Moreover, the residual

depths reported after complete unload showed that addition of hybrid precursor also made the coatings more elastic which explains the better scratch resistance of these latter.

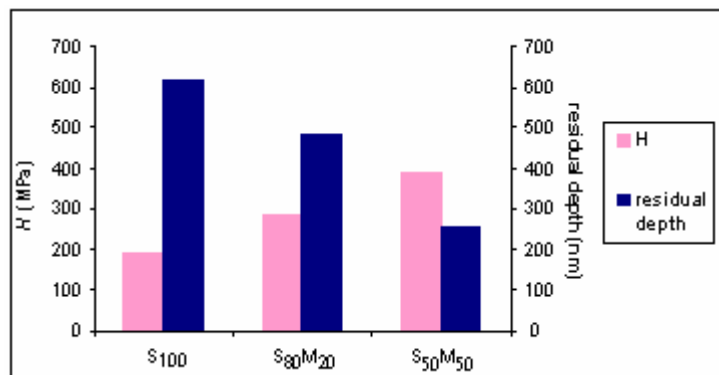


Figure 2: Hardness H and residual depth after nanoindentation tests performed onto S₁₀₀, S₈₀M₂₀ and S₅₀M₅₀ UV-cured coatings.

IV. Conclusion

A wide range of solid cross-linked organic-inorganic coatings were obtained in one step, through UV-curing of ambifunctional hybrid precursors used alone or mixed with an organic resin in presence of a diaryl iodonium salt. The build up of the inorganic network was catalyzed by the photogenerated acids while the organic chains were created either by a cationic PI or by a radical PI (according to the organic moiety functionality). FTIR and NMR spectroscopies enable a deep understanding of the simultaneous organic-inorganic photopolymerization. Thermo-mechanical characterization led to the conclusion that the addition of hybrid precursors to organic resins resulted in the densification of the hybrid network crosslinking due to the inorganic part contribution. In addition, an increase in the glass transition temperature, in the hardness and in the viscoelastic properties of the cured films was observed thus resulting in the improvement of their scratch resistance. This single step method appeared to be particularly advantageous in terms of rapidity, efficiency, absence of solvent and low energy consumption and opens up new opportunities in the UV-cured coatings field. Indeed, it is thus possible to modulate the structural and mechanical properties of the resulting nanocomposite coatings by changing either the nature or concentration of the hybrid precursor.

V. References

- 1 Etienne, P.; Coudray, P.; Moreau, Y.; Porque, J.; J Sol-Gel Sci Technol 1998, 13, 523.
- 2 Oubaha, M.; Kribich, R. K.; Copperwhite, R.; Etienne, P.; O'Dwyer, K.; MacCraith, B. D.; Moreau, Y.; Opt Commun 2005, 253, 346.
- 3 Fardad, A.; Andrews, M.; Milova, G.; Malek-Tabrizi, A.; Najafi, I.; Appl Opt 1998, 37, 2429.
- 4 Croutxé-Barghorn, C.; Soppera, O.; Chevallier, M.; Macromol Mater Eng 2003, 288, 219.
- 5 Gilberts, J.; Tinnemans A.H.A.; Hogerheide M.P.; Koster T.P.M.; J Sol-Gel Sci Technol, 1998, 11(2), 153.
- 6 Schottner, G.; Rose K.; Posset U.; J Sol-Gel Sci Technol, 2003, 27(1), 71.
- 7 Amberg-Schwab, S.; Katschorek H.; Weber U.; Hoffmann, Burger A.; J Sol-Gel Sci Technol, 2003, 26(1), 699.
- 8 Soucek, M.D.; Zong Z.; Johnson A.J.; JCT Res, 2006, 3(2), 133.
- 9 Sangermano, M.; Borlatto E.; D'Hérin Bytner F.D.; Priola A.; Rizza G.; Prog Org Coat, 2007, 59(2), 122.
- 10 Croutxé-Barghorn, C.; Soppera, O.; Carre, C.; J Sol-Gel Sci Technol 2007, 41, 93.
- 11 Feuillade, M.; Croutxé-Barghorn, C.; Carre, C.; Prog Solid State Chem 2006, 34, 87.
- 12 Brusatin, G.; Giustina G.D.; Guglielmi M.; Innocenzi P.; Prog Solid State Chem, 2006, 34(2-4), 223.
- 13 Crivello, J.V.; Song K.Y.; Ghoshal R.; Chem Mater, 2001, 13(5), 1932.
- 14 Crivello, J. V.; Bi, D.; Lu, Y.; Macromol Symp 1995, 95, 79.
- 15 Soucek, M. D.; Johnson, A. H.; Meemken, L. E.; Wegner, J. M.; Polym Adv Technol 2005, 16, 257.
- 16 Chemtob, A.; Versace, D.-L.; Belon, C.; Croutxé-Barghorn, C.; Rigolet, S. ; Macromolecules 2008, 41, 7390.
- 17 Gauthier, C.; Lafaye, S.; Schirrer, R.; Tribol Int 2001, 34, 469.